

1 **Fluctuation-Dissipation Supplemented by Nonlinearity:**

2 **A Climate-Dependent Sub-Grid-Scale Parameterization in**

3 **Low-Order Climate Models**

4 ULRICH ACHATZ ^{*}, ULRIKE LÖBL [†], AND STAMEN I. DOLAPTCHIEV

Institut für Atmosphäre und Umwelt, Goethe-Universität Frankfurt, Frankfurt am Main, Germany

5 ANDREY GRITSUN

Institute of Numerical Mathematics, Moscow, Russia

^{*} *Corresponding author address:* Ulrich Achatz, Institut für Atmosphäre und Umwelt, Goethe-Universität Frankfurt, Altenhöferallee 1, D-60438 Frankfurt am Main, Germany.

E-mail: achatz@iau.uni-frankfurt.de

[†] *Now at:* Institut für Geowissenschaften, Goethe-Universität Frankfurt, Frankfurt am Main, Germany

ABSTRACT

7 Climate system models use a multitude of parameterization schemes for small-scale pro-
8 cesses. These should respond to externally forced climate variability in an appropriate man-
9 ner so as to reflect the response of the parameterized process to a changing climate. The
10 most attractive route to achieve such a behavior would certainly be provided by theoretical
11 understanding sufficiently deep to enable the à-priori design of climate-sensitive parameteri-
12 zation schemes. An alternative path might, however, be helpful when the parameter tuning
13 involved in the development of a scheme is objective enough so that these parameters can be
14 described as functions of the statistics of the climate system. Provided that the dynamics
15 of the process in question is sufficiently stochastic, and that the external forcing is not too
16 strong, the fluctuation-dissipation theorem (FDT) might be a tool to predict from the statis-
17 tics of a system (e.g. the atmosphere) how an objectively tuned parameterization should
18 respond to external forcing (e.g. by anomalous sea-surface temperatures). This problem is
19 addressed within the framework of low-order (reduced) models for barotropic flow on the
20 sphere, based on a few optimal basis functions and using an empirical linear sub-grid-scale
21 (SGS) closure. A reduced variant of quasi-Gaussian FDT (rqG-FDT) is used to predict the
22 response of the SGS closure to anomalous local vorticity forcing. At sufficiently weak forcing
23 use of the rqG-FDT is found to systematically improve the agreement between the response
24 of a reduced model and that of a classic spectral code for the solution of the barotropic
25 vorticity equation.

26 1. Introduction

27 Both curse, challenge and beauty of atmospheric dynamics is the enormous range of
28 scales involved. Beginning with planetary-scale climate-variability patterns, it extends over
29 synoptic-scale weather and mesoscale systems, such as fronts or gravity waves, down to
30 turbulence on the millimeter scale. Understanding the interactions between these various
31 scales is both a daunting task and a necessity for faithful climate modeling. As has been
32 argued by Held (2005) a hierarchy of models, from full-fledged climate-system models (CSM)
33 down to conceptual models, is needed to gain and keep overview in this complex setting,
34 and thus go on making progress in climate research as a whole. The basis for typical con-
35 ceptional modeling of atmosphere or ocean dynamics is some kind of filtering. The most
36 classical example is quasigeostrophic theory (Charney 1948), providing the basis for cor-
37 responding multi-layer models (Phillips 1954, 1956) as have been applied, e.g., in climate
38 modeling by Opsteegh et al. (1998). Others are soundproof approximations of atmospheric
39 dynamics (Ogura and Phillips 1962; Lipps and Hemler 1982; Lipps 1990; Durran 1989),
40 or the planetary-geostrophic approximation (Robinson and Stommel 1959; Welander 1959;
41 Phillips 1963) which is at the heart of representative earth system models of intermediate
42 complexity (e.g. Petoukhov et al. 2000). An especially compact approach is represented by
43 deterministic low-order models based on some kind of optimal basis patterns (e.g. Selten
44 1995; Achatz et al. 1995; Kwasniok 1996; Achatz and Schmitz 1997; Selten 1997; Achatz
45 and Branstator 1999; Achatz and Opsteegh 2003a,b; Kwasniok 2004, 2007). Although these
46 have been shown to reproduce various aspects of internal climate variability, they have not
47 yet found their way into practical climate modeling.

48 Common to both conceptual and full-fledged climate models (even the latter are there-
49 fore in some regard conceptual) is that they do not resolve certain small-scale structures
50 or processes (e.g. synoptic-scale or mesoscale systems, clouds etc.) which yet have a non-
51 negligible feedback on the resolved scales. That feedback must be taken into account via
52 suitably formulated sub-grid-scale (SGS) parameterizations. Regardless whether these are

53 given a stochastic (e.g. Hasselmann 1976; Farrell and Ioannou 1993, 1996a,b; Majda et al.
54 2003; Franzke et al. 2005; Franzke and Majda 2006; Dolapchiev et al. 2012) or deterministic
55 formulation, nonlinearity and general complexity of the processes in question have so far
56 always prevented a complete à-priori derivation from first principles. The common approach
57 is data driven, i.e. some assumption is made about the functional form of the parameter-
58 ization, often based on some theory, and the corresponding parameters are obtained in a
59 more or less objective manner by tuning against some reference data set. The crudeness in
60 this procedure varies widely. At one end one might see traditional damping by some hyper-
61 diffusivity, typically tuned via eye-ball comparisons of simulated mean fields or fluxes. A
62 sophisticated approach is stochastic mode reduction suggested by Majda et al. (2003) where
63 the nonlinear self-interaction of unresolved scales is given an empirical description by an
64 Ornstein-Uhlenbeck process which is then used for an explicit derivation of the stochastic
65 SGS parameterization. Somewhat of a middle route is perhaps represented by Achatz and
66 Branstator (1999) who use an empirical linear SGS closure where the parameters have been
67 chosen so as to minimize the mean error between resolved tendencies either predicted by the
68 model or measured in a reference data set, there from an atmospheric general circulation
69 model (GCM).

70 A perhaps prototypical problem of empirical SGS schemes is confronting Achatz and
71 Branstator (1999): Their low-order models, based on a limited number of empirical orthog-
72 onal functions (EOF), simulate the GCM climate very well. Nonetheless they seem to fail
73 to reproduce the climate response of the GCM to some local anomalous thermal forcing. An
74 explanation for this could have been that the nonlinear dynamics of the low-order model,
75 obtained from a projection of the equations of a quasigeostrophic two-layer model onto the
76 EOFs, was too simple. However, analogous attempts by Achatz and Opsteegh (2003a,b),
77 now using primitive equation dynamics, did not solve the problem. Again the GCM climate
78 was simulated well, again the anomalous response to local thermal forcing could not be re-
79 produced to a satisfactory degree. Still a possible explanation could be that the dynamics

80 of the low-order model, using the dry primitive equations on three layers, is too far away
81 from that of the much more sophisticated 19-level GCM (described by Voss et al. 1998).
82 The problem might, however, be deeper and more general than that: as the SGS-scheme
83 parameters have been determined by tuning against the unperturbed GCM climate, and as
84 that works so well, it might be that an SGS scheme tuned à-posteriori against the perturbed
85 climate could enable the low-order model to reproduce the anomalous response. In other
86 words, the SGS closure should be formulated climate dependent. This is perhaps a problem
87 to be faced by many SGS parameterizations in climate models: The less they are based on
88 first principles, and the more they rely on tuning against present-day or past climate, the
89 more they might be in danger of failing in a changing climate.

90 The ideal approach to tackle this problem would be the development of SGS schemes
91 based sufficiently on first principles so that the empirical parameters do not matter that
92 much anymore. Perhaps stochastic mode reduction (Majda et al. 2003; Dolaptchiev et al.
93 2012) points into a direction helping under some circumstances, as is also suggested by Majda
94 et al. (2010) who show a reduced stochastic model of a three-component system to exhibit a
95 realistic response to external perturbations. One might also reconsider the tuning processes
96 for the SGS parameterization. The minimization of relative entropy between the statistics
97 of low-order model and GCM might lead to reduced models with a more faithful climate
98 sensitivity (Majda and Gershgorin 2010, 2011a,b; Branicki and Majda 2012). However, we
99 here follow another route. As long as the parameter tuning implies the minimization of some
100 objectively formulated error, e.g. in predicted tendencies, between model and reference data
101 set, a reasonable à-priori estimate of the change in the corresponding statistics could help.
102 Fortunately, under certain conditions such an estimate can be obtained from the fluctuation-
103 dissipation theorem (Deker and Haake 1975; Hänggi and Thomas 1977; Risken 1984; Gritsun
104 2001; Gritsun et al. 2002; Gritsun and Branstator 2007; Abramov and Majda 2009; Majda
105 et al. 2010; Cooper and Haynes 2011). For an analysis of the potential of this approach
106 we have restrained ourselves to a minimal framework we hoped to contain all necessary

107 ingredients. Instead of a full-fledged GCM, or even real climate data, we use a spectral
 108 code for the barotropic vorticity equation on the sphere as toy atmosphere, construct a
 109 low-order model based on EOFs (Selten 1995), and use the empirical SGS parameterization
 110 as proposed by Achatz and Branstator (1999). Our results indicate that the fluctuation
 111 dissipation theorem (FDT) is not only able to improve the performance of the low-order
 112 model in simulating the response to anomalous vorticity forcing, but that the corresponding
 113 prediction is also better than that from the most frequently used quasi-Gaussian variant of
 114 the FDT itself.

115 The manuscript is structured as follows: Section 2 describes the toy atmosphere, the
 116 approach for construction of a low-order model for its simulation, and some characteristics
 117 of the latter. Section 3 gives an account of how we use the FDT for formulating the climate
 118 dependence of the SGS closure of the low-order model, while section 4 presents results on how
 119 well this approach works for the simulation of the response to anomalous vorticity forcing.
 120 Finally we summarize and discuss our findings in section 5.

121 **2. Toy atmosphere and low-order climate model**

122 *a. Toy atmosphere*

123 The toy atmosphere used here is a spectral code (Selten 1995) for the solution of the
 124 barotropic vorticity equation

$$\frac{\partial \nabla^2 \psi}{\partial t} + J\left(\psi, \nabla^2 \psi + f + f_0 \frac{h}{H}\right) = -k_E \nabla^2 \psi - k_h \nabla^6 \psi + F \quad (1)$$

125 on the sphere. Here ψ is the streamfunction, J the standard Jacobian operator, f the
 126 Coriolis parameter, f_0 a midlatitude value of the latter (at 45°N), h/H a normalized envelope
 127 orography, k_E represents Ekman damping (with a time scale of 15d), k_h is the hyper-diffusion
 128 coefficient (damping the shortest total wavelengths with a time scale of 3d), and F is a forcing
 129 tuned by Franzke et al. (2005) so as to lead to a model variability as representative of available

130 northern-hemisphere analysis data as possible. The spherical-harmonic expansion of the
 131 streamfunction is truncated in a triangular manner at T21. Since the model is constrained
 132 to be symmetric with respect to the equator it has $N = 231$ degrees of freedom, i.e. non-zero
 133 vorticity spectral coefficients where real and imaginary parts count separately. Gathering
 134 these in a state vector $\mathbf{x} \in \mathbb{R}^N$, the dynamical equation of our toy atmosphere can be written

$$\frac{d\mathbf{x}}{dt} = \mathbf{G}(\mathbf{x}) \quad (2)$$

135 where \mathbf{G} is the appropriate function.

136 *b. Low-order climate model*

137 Instead of spherical harmonics our low-order climate model uses as basis functions em-
 138 pirical orthogonal functions (EOF). These have been extracted from data from 200000d of
 139 our toy atmosphere. An energy metric has been employed (Selten 1995) for this so that the
 140 norm

$$\begin{aligned} |\mathbf{x}|^2 &= a^2 \int_0^{2\pi} d\lambda \int_{-\pi/2}^{\pi/2} d\phi \cos \phi |\nabla \psi|^2 \\ &= \sum_{m=1}^{21} \sum_{n=m}^{21} n(n+1) |\psi_{mn}|^2 = \mathbf{x}^t \mathbf{M} \mathbf{x} \end{aligned} \quad (3)$$

141 is proportional to the total energy of the flow, where a is the radius of the earth, λ and ϕ
 142 geographic longitude and latitude, and ψ_{mn} a spectral coefficient at zonal and total wavenum-
 143 bers m and n . The corresponding metric \mathbf{M} is an $N \times N$ -dimensional real symmetric matrix.
 144 We found that 43 EOFs suffice to explain more than 90% of the variance in the analyzed
 145 data. In general, if M leading EOFs are chosen to approximate the state vector, the latter
 146 can be written

$$\mathbf{x} = \langle \mathbf{x} \rangle + \mathbf{P} \mathbf{a} + \varepsilon \quad (4)$$

147 where angle brackets indicate the time mean, \mathbf{P} is an $N \times M$ -matrix containing the EOFs
 148 as columns, $\mathbf{a} \in \mathbb{R}^M$ is the vector of EOF expansion coefficients (the principal components),

149 and ε the time dependent truncation error. The latter is orthogonal to the EOFs so that
 150 the principal components can be determined from the data via

$$\mathbf{a} = \mathbf{P}^t \mathbf{M} \mathbf{x}' \quad (5)$$

151 where a prime indicates deviations from the mean, i.e. here $\mathbf{x}' = \mathbf{x} - \langle \mathbf{x} \rangle$.

152 Taking the time derivative, and using the dynamical equation (2) of the toy atmosphere
 153 together with the reduced representation (4) one gets

$$\frac{d\mathbf{a}}{dt} = \mathbf{P}^t \mathbf{M} \mathbf{G} (\langle \mathbf{x} \rangle + \mathbf{P} \mathbf{a}) + \mathbf{s}(\mathbf{x}, \mathbf{a}) \quad (6)$$

154 where \mathbf{s} is the SGS error arising from the neglect of the truncation error inside \mathbf{G} . A
 155 low-order climate model for \mathbf{a} is obtained by replacing the SGS error by a suitably chosen
 156 parameterization $\mathbf{p}(\mathbf{a})$. The model equations are then

$$\left(\frac{d\mathbf{a}}{dt} \right)_M = \mathbf{P}(\mathbf{a}) + \mathbf{p}(\mathbf{a}) \quad , \quad (7)$$

157 the shortcut $\mathbf{P}(\mathbf{a}) = \mathbf{P}^t \mathbf{M} \mathbf{G} (\langle \mathbf{x} \rangle + \mathbf{P} \mathbf{a})$ indicating the projected model without SGS param-
 158 eterization. Note that the (toy) atmosphere data do not satisfy (7) but rather

$$\frac{d\mathbf{a}}{dt} = \mathbf{P}(\mathbf{a}) + \mathbf{p}(\mathbf{a}) + \varepsilon_p(\mathbf{x}, \mathbf{a}) \quad , \quad (8)$$

159 with a parameterization error $\varepsilon_p(\mathbf{x}, \mathbf{a}) = \mathbf{s}(\mathbf{x}, \mathbf{a}) - \mathbf{p}(\mathbf{a})$. Following Achatz and Branstator
 160 (1999) we now choose a linear parameterization

$$\mathbf{p}(\mathbf{a}) = \mathbf{F} + \mathbf{L} \mathbf{a} \quad (9)$$

161 and, instead of tuning the vector \mathbf{F} and the matrix \mathbf{L} by test integrations and eyeball fits of
 162 the climate-model climatology, we determine them by the requirement that, averaged over
 163 the available data, the norm of the parameterization error is to be as small as possible. This
 164 amounts to the solution of a linear regression problem, yielding

$$\mathbf{L} = \langle \mathbf{s}' \mathbf{a}'^t \rangle \langle \mathbf{a}' \mathbf{a}'^t \rangle^{-1} \quad (10)$$

$$\mathbf{F} = \langle \mathbf{s} \rangle - \mathbf{L} \langle \mathbf{a} \rangle \quad . \quad (11)$$

165 This way the SGS-closure parameters in (9) are determined from the climate statistics of the
 166 toy atmosphere. Necessary input are the covariance $\langle \mathbf{s}' \mathbf{a}'^t \rangle$ between SGS error \mathbf{s} and the state
 167 vector \mathbf{a} modeled by the climate model, the auto-covariance $\langle \mathbf{a}' \mathbf{a}'^t \rangle$ of the latter, its mean
 168 $\langle \mathbf{a} \rangle$, and the mean SGS error $\langle \mathbf{s} \rangle$. Fig. 1 shows mean streamfunction and streamfunction
 169 variance from daily data from 200000d of the toy atmosphere, and the corresponding results
 170 from low-order models based on 40 EOFs, either without or with SGS parameterization.
 171 The improvement achieved by the parameterization is evident.

172 **3. Climate dependent SGS closure by the fluctuation-** 173 **dissipation theorem**

174 *a. External forcing*

175 The question now is whether the low-order climate model can respond correctly to some
 176 external atmospheric forcing. As in Achatz and Branstator (1999) and Achatz and Opsteegh
 177 (2003b) we choose a local forcing. However, since the variability of the toy atmosphere is
 178 low close to the equator, and thus the leading EOFs would not be well able to represent a
 179 tropical forcing, we have rather chosen to place it at midlatitudes. The vorticity forcing is
 180 of the form

$$\delta F_\zeta = A \cdot 5 \cdot 10^{-6} f \cos^2 \left(\frac{\lambda - \lambda_c}{\Delta \lambda} \right) \cos^2 \left(\frac{\phi - \phi_c}{\Delta \phi} \right) \quad (12)$$

181 The scaling has been chosen so that the anomalous forcing is at $A = 1$ of the same order as
 182 the climatological forcing, i.e. $\delta F_\zeta / F = O(1)$. In all experiments to be discussed here the
 183 forcing is centered at latitude $\phi_c = 45^\circ$, its width is $\Delta \lambda = \Delta \phi = 20^\circ$, and it has amplitude
 184 $A = 0.1$. In total we will base our conclusions on experiments with center longitude of the
 185 forcing being at $\lambda_c = 0^\circ, 30^\circ, \dots, 330^\circ$. It has always been projected on the same EOFs as
 186 the corresponding low-order climate models are using. As an example we show in Fig. 2 the
 187 case $\lambda_c = 180^\circ$, either total, projected onto 40 EOFs, or projected onto 90 EOFs.

188 *b. Fluctuation-dissipation theorem*

189 The external forcing changes the statistics of the toy atmosphere so that a low-order
 190 climate model should incorporate this effect in predicting the atmosphere response to the
 191 forcing. In principle, one can always do the experiment and obtain a perturbed closure à-
 192 posteriori from data from the perturbed climate, using (10) and (11). The perturbed model
 193 would then be

$$\frac{d\mathbf{a}}{dt} = \mathbf{P}(\mathbf{a}) + \mathbf{F} + \mathbf{L}\mathbf{a} + \delta\mathbf{F} + \delta\mathbf{L}\mathbf{a} + \mathbf{P}^t\mathbf{M}\delta\mathbf{F}_\zeta \quad (13)$$

194 where $\mathbf{P}^t\mathbf{M}\delta\mathbf{F}_\zeta$ represents the anomalous-forcing spectral coefficients projected onto the
 195 EOFs, and

$$\delta\mathbf{L} = \delta(\langle \mathbf{s}'\mathbf{a}'^t \rangle \langle \mathbf{a}'\mathbf{a}'^t \rangle^{-1}) \quad (14)$$

$$\delta\mathbf{F} = \delta\langle \mathbf{s} \rangle - \delta(\mathbf{L}\langle \mathbf{a} \rangle) \quad (15)$$

196 are the corrections in the closure due to the changing climate. Obviously this à-posteriori
 197 tuning would make the low-order model useless. Only if the changing statistics can be
 198 predicted before-hand this would be a viable option.

199 Fortunately, the fluctuation-dissipation theorem (Kraichnan 1959; Risken 1984) offers a
 200 way how this prediction could be done approximately, albeit under certain assumptions. It
 201 considers either a deterministic system governed by

$$\frac{d\mathbf{x}}{dt} = \mathbf{A}(\mathbf{x}, t) \quad (16)$$

202 or a stochastic system controlled by the corresponding stochastic differential equation

$$d\mathbf{x} = \mathbf{A}(\mathbf{x}, t) dt + \mathbf{B}(\mathbf{x}, t) d\mathbf{W} \quad (17)$$

203 where \mathbf{x} is the state vector of the system, here of the (toy) atmosphere, \mathbf{A} is the deterministic
 204 drift, \mathbf{B} the diffusion tensor, and $d\mathbf{W}$ a multidimensional Wiener process. The applicability
 205 of the FDT to deterministic systems is often hampered by the fractality of the corresponding
 206 probability-density function (PDF). In such cases it can help to add a small noise term, as in

207 (17), to ensure that the PDF is sufficiently smooth (Zeeman 1988). In our application here,
 208 e.g., the underlying system is not stochastic, but we assume that the nonlinear dynamics
 209 of the smallest-scale processes acts in a sufficiently irregular manner so that stochasticity
 210 is a reasonable approximation. To proceed, the general FDT predicts the response of the
 211 statistics of the system to an *infinitesimally small perturbation* $\delta\mathbf{f}(\mathbf{x}, t)$ of the drift vector so
 212 that

$$\mathbf{A}(\mathbf{x}, t) \rightarrow \mathbf{A}(\mathbf{x}, t) + \delta\mathbf{f}(\mathbf{x}, t) \quad . \quad (18)$$

213 It provides an estimate of the change in the expectation of any observable $\mathbf{h}(\mathbf{x})$, i.e. of

$$\langle \mathbf{h} \rangle (t) = \int d^N x p(\mathbf{x}, t) \mathbf{h}(\mathbf{x}) \quad (19)$$

214 where p is the PDF. This is also the situation encountered in our problem. Due to (5) and
 215 $\mathbf{s} = \mathbf{s}(\mathbf{x}, \mathbf{a})$ all the climate means needed for the determination of the SGS closure parameters
 216 in (11) and (10) are expectations of suitably defined observables $\mathbf{h}(\mathbf{x})$. Quasi-Gaussian FDT
 217 (qG-FDT), the most frequently used variant of FDT assumes that the equilibrium PDF is
 218 Gaussian. This is a certain restriction. Cooper and Haynes (2011) suggest how to relax
 219 it by estimating the equilibrium PDF by a kernel method. An alternative, not inherently
 220 restricted to low-dimensional applications as there, is the blended short-time/quasi-Gaussian
 221 FDT method (ST/qG-FDT) developed by Abramov and Majda (2009). This approach,
 222 superior to qG-FDT, uses a tangent linear model to determine the short-time response to
 223 external forcing, combined with qG-FDT for longer response times. For the time being,
 224 however, we want to stick with qG-FDT, since it is more easily implemented than ST/qG-
 225 FDT and since it typically requires considerably less reference data than kernel methods.
 226 Under the assumption of Gaussianity the predicted *steady-state response* for $t \rightarrow \infty$ to an
 227 *anomalous forcing*

$$\delta\mathbf{f}(\mathbf{x}, t) = \delta\mathbf{f}(t) \quad (20)$$

228 is

$$\lim_{t \rightarrow \infty} \delta\langle \mathbf{h} \rangle (t) = \lim_{t \rightarrow \infty} \int_0^t d\tau \langle \mathbf{h}[\mathbf{X}(\tau)] \mathbf{X}^t(0) \rangle \langle \mathbf{x}' \mathbf{x}'^t \rangle^{-1} \delta\mathbf{f}(t - \tau) \quad (21)$$

229 which yields for constant forcing, as here,

$$\lim_{t \rightarrow \infty} \delta \langle \mathbf{h} \rangle (t) = \mathbf{R} \delta \mathbf{f} \quad , \quad (22)$$

230 with qG-FDT response operator

$$\mathbf{R} = \int_0^\infty d\tau \langle \mathbf{h} [\mathbf{X}(\tau)] \mathbf{X}^t(0) \rangle \langle \mathbf{x}' \mathbf{x}^t \rangle^{-1} \quad (23)$$

231 The task is to determine the integral over all time lags of the lagged covariance between
 232 the observable and the state vector, multiplied by the inverse of the lag-zero auto-covariance
 233 matrix. This offers a way for the determination of the response of all SGS closure parameters
 234 in (11) and (10), or rather of the expectations $\langle \mathbf{a} \rangle$, $\langle \mathbf{s} \rangle$, $\langle \mathbf{s}' \mathbf{a}^t \rangle$, and $\langle \mathbf{a}' \mathbf{a}^t \rangle$ required for their
 235 calculation.

236 *c. Reduced quasi-Gaussian FDT*

237 Referring to (10) and (11) we note again that the observables we need modified means
 238 for are the reduced state vector \mathbf{a} , the SGS error \mathbf{s} , the matrix $\mathbf{s}' \mathbf{a}^t$ yielding in the mean the
 239 covariance of the SGS error with the reduced state vector, and the matrix $\mathbf{a}' \mathbf{a}^t$ averaging
 240 to the auto-covariance. The ability of qG-FDT to predict the atmospheric response in these
 241 observables has been estimated by performing 12 experiments with a mid-latitude anomalous
 242 forcing with amplitude $A = 0.1$ at longitudes $\lambda_c = 0^\circ, 30^\circ, \dots, 330^\circ$, and projected onto the
 243 leading 40 EOFs. Each case has been integrated for 200000d. A reference case has been
 244 obtained by integrating the model over 500000d, and the qG-FDT response operator has
 245 been approximated by integrating the lagged covariances in the reference data over 50d. For
 246 this a simple Riemann sum has been used, with a time step of 1d. Following Gritsun and
 247 Branstator (2007) and Majda et al. (2010) we have not determined the operator in the full
 248 state space but rather in the state space spanned by the leading 40 EOFs. The estimate of
 249 the response in the four quantities in question has then been obtained using qG-FDT, and
 250 that has been compared to the true response from the toy atmosphere. The comparison has

251 been made by calculating a relative error in EOF space, defined, either for two vectors \mathbf{a} and
 252 \mathbf{b} , or for two matrices \mathbf{A} and \mathbf{B} , as

$$\epsilon = \begin{cases} \frac{|\mathbf{a} - \mathbf{b}|^2}{|\mathbf{a}| |\mathbf{b}|} \\ \frac{|\mathbf{A} - \mathbf{B}|^2}{|\mathbf{A}| |\mathbf{B}|} \end{cases} \quad (24)$$

253 where the norm of a matrix is taken to be the Frobenius norm, i.e. the square root of the
 254 squared sum of matrix elements. Pattern correlations, not shown here, have been calculated
 255 as well, without yielding any further insights.

256 The results are shown in Fig. 3. With the one exception of the forcing located at
 257 $\lambda_c = 270^\circ$, the anomalous first moments $\langle \mathbf{a} \rangle$ and $\langle \mathbf{s} \rangle$ are predicted by qG-FDT with an error
 258 less than 1, whereas the second moments $\langle \mathbf{s}' \mathbf{a}'^t \rangle$ and $\langle \mathbf{a}' \mathbf{a}'^t \rangle$ are not predicted so well. This
 259 implies that the prediction of the change in the linear operator of the SGS closure, using (14),
 260 could be flawed. As Fig. 4 shows, this is indeed the case. The error between the change either
 261 estimated from qG-FDT or obtained à-posteriori from the data of the perturbed atmosphere
 262 is always of order 1 or larger. The same holds for the prediction of the change of the forcing
 263 of the SGS parameterization, using (15), since it uses the ill-estimated $\delta \mathbf{L}$.

264 It turns out, however, that if $\delta \mathbf{L}$ is neglected, a useful estimate of $\delta \mathbf{F}$ can be obtained.
 265 This *reduced quasi-Gaussian FDT (rqG-FDT)* uses

$$\delta \mathbf{L} = 0 \quad (25)$$

$$\delta \mathbf{F} = \delta \langle \mathbf{s} \rangle - \mathbf{L} \delta \langle \mathbf{a} \rangle \quad , \quad (26)$$

266 Its quality is shown in Fig.4 as well. Cases of anomalous vorticity forcings projected on more
 267 or less EOFs (20, 30, ..., 90), and low-order models of corresponding resolution have been
 268 investigated as well, indicating a general potential of reduced qG-FDT to make a useful
 269 prediction of the anomalous SGS forcing. The 90-EOF case, e.g., investigated below in
 270 somewhat greater detail, shows the same qualitative results as the 40-EOF case discussed
 271 here. Therefore our method of choice applied below is rqG-FDT.

272 4. Results

273 The utility of reduced qG-FDT is eventually decided by its ability to help a low-order
274 climate model in simulating the atmospheric response to anomalous vorticity forcing. Our
275 respective results will first be illustrated using a representative example. This is the case of
276 anomalous forcing at longitude $\lambda_c = 210^\circ$ projected onto 90 EOFs. Fig. 5 shows the mean-
277 streamfunction response of the toy atmosphere to this forcing, the corresponding response
278 from three different 90-EOF models, and that predicted by qG-FDT. The low-order climate
279 model CM0 uses an unmodified SGS parameterization, the model CMP applies a parameter-
280 ization modified à-posteriori by a new determination of the SGS-model parameters from the
281 perturbed atmosphere, and the model CMF uses a parameterization modified before-hand
282 via reduced qG-FDT. This is also compared to the direct prediction of the streamfunction
283 response by qG-FDT. The atmospheric response has a strong zonal component with maxima
284 over the pole and in the subtropics, and a minimum in midlatitudes. A wave component
285 exhibits a maximum over the subtropical Pacific, and three minima over the midlatitude
286 Pacific and Atlantic ocean and over Siberia. This pattern is reproduced quite well even by
287 CM0. The relative error in the simulated response is 0.124. CMF brings an improvement,
288 e.g. over the Pacific, so that the relative error drops to 0.058. This is even better than the
289 direct qG-FDT result which has a relative error of 0.228. For better orientation Fig. 6 shows
290 the change in the mean zonal wind, exhibiting an intensification and eastward shift of the
291 two jet streams. Maximum values are about 9m/s. This is of the same order as zonal-mean
292 zonal wind changes in present-day simulations of anthropogenic climate change (e.g. Lorenz
293 and DeWeaver 2007). Notwithstanding its linear nature rqG-FDT is able to predict the
294 change in the SGS parameterization well enough that model CMF can simulate that mean
295 zonal-wind change faithfully.

296 As discussed in subsection 3c, standard qG-FDT is well able to predict the change in first
297 moments of the atmosphere. This is also visible in the results shown so far. Second moments,
298 however, had been shown to be more difficult an object for qG-FDT. This is born out in Fig.

299 7, where the response in the streamfunction variance is shown. qG-FDT predicts a signal
300 which is considerably too strong (relative error 2.47). Here the nonlinear models perform
301 better, especially if supplemented by a rqG-FDT modification of the SGS parameterization.
302 The predicted response is slightly too weak, but the predicted pattern is matched very well,
303 with an increase of variance over the pole, and north and south of the jet streams. The
304 relative errors are 0.527 for CM0 and 0.342 for CMF.

305 Relative errors, yielding a quantitative estimate of the quality of the simulated response,
306 have not just been calculated for an anomalous forcing at longitude $\lambda_c = 210^\circ$, but for all
307 twelve cases examined. Fig. 8 shows the relative errors in the predictions of the change in
308 the first moments. With the exception of the three cases with forcing longitude between 210°
309 and 270° , qG-FDT is better able to predict the response than the unmodified climate model.
310 Only in four out of the twelve cases ($\lambda_c = 60^\circ, 180^\circ, 300^\circ$ and 330°), however, rqG-FDT is
311 not able to improve the climate model so much that it can outdo qG-FDT. The balance in
312 favor of climate models supplemented by rqG-FDT becomes even more convincing in the
313 case of the second moments, shown in Fig. 9. Here it is always the climate model using rqG-
314 FDT for the adjustment of the SGS parameterization that gives the better prediction. Note
315 also that the model with SGS parameterization modified à-posteriori is always performing
316 best. Although this model is useless in itself, this fact demonstrates that there might be even
317 more potential in the approach, should it become possible to also predict the second-moment
318 change better than qG-FDT is able to.

319 Finally, we give an overview how our results depend on the number of EOFs which the
320 anomalous forcing and the climate models are based on. This is to give an indication on
321 how well the approach might work at various conceivable levels of climate-model simplicity in
322 comparison with the true complexity of the atmosphere. For this purpose, we have calculated,
323 for either the first- or second-moment errors, a mean over all twelve cases and a root-mean-
324 square deviation. Mean plus/minus r.m.s. deviation of the first-moment errors are shown in
325 Fig. 10 for models based on between 20 and 90 EOFs. The smallest models, based on only 20

326 EOFs, are performing worse than the qG-FDT, even if the SGS parameterization is adjusted
327 à-posteriori. At model resolutions too coarse the linear ansatz for the SGS parameterization
328 cannot compete with qG-FDT. This already changes, however, at a resolution of 30 EOFs.
329 At this and all higher resolutions simulations by an optimally adjusted nonlinear climate
330 model can outperform direct application of qG-FDT. Nonetheless, application of rqG-FDT
331 helps to improve the model behavior at all examined resolutions. Models based on 60 or 70
332 EOFs become as good as qG-FDT if rqG-FDT is used to adjust the parameterization, and
333 at higher resolutions they perform better. This gain becomes even more obvious as one looks
334 at the second moments. Fig. 11 shows the weakness of qG-FDT in predicting the anomaly
335 in these, but also that the climate-model simulations can yield useful results, especially
336 for models with higher resolution and supplemented by rqG-FDT. The modification of the
337 SGS parameterization by rqG-FDT gives an approximate net 30% improvement over models
338 without modified parameterization, and considerably more over the direct application of
339 qG-FDT, when 80 or 90 EOFs are used.

340 5. Summary and discussion

341 We have addressed the question how sub-grid-scale (SGS) parameterizations in climate
342 models can be formulated so that they respond correctly to an externally forced change in
343 climate statistics. For this purpose we have considered a toy atmosphere represented by a
344 spectral code, with resolution T21, for the solution of the barotropic vorticity equation on
345 the sphere. The vorticity forcing in that code has been chosen so that its climate exhibits a
346 certain similarity to that of the real atmosphere. Low-order climate models have then been
347 constructed which are based on empirical orthogonal functions (EOF). For this an energy
348 metric has been used. The identified variance spectrum is relatively flat. About 40 basis
349 patterns are needed for representing 90% of the total variance of the toy atmosphere. The
350 dynamical equations of the climate models, varying by the number of EOFs they are based

351 on, have been obtained by projecting the T21 code for the barotropic vorticity equation onto
352 the EOFs, and by adding an SGS parameterization which is to describe the feedback from
353 unresolved modes. That parameterization has been given a formulation which is linear in
354 terms of the EOF expansion coefficients. The respective parameters, comprised in an SGS
355 forcing and a linear SGS operator, have been determined from the toy-atmosphere climate in
356 such a manner that the residual error between modeled and measured tendencies, averaged
357 over all available climate data, is as small as possible. This represents an objective tuning
358 process.

359 Parameters of an SGS parameterization tuned at present-day climate might have to
360 respond to climate change. We suggest that the fluctuation-dissipation theorem (FDT)
361 is used to predict this response. Corresponding response operators have been constructed
362 from the toy-atmosphere climate data, assuming their probability-density function (PDF)
363 to be Gaussian (qG-FDT). This is a limiting assumption which one could potentially relax.
364 A more general treatment would, however, either necessitate the estimate of the PDF by
365 kernel methods (Cooper and Haynes 2011) or require the use of a tangent-linear model for
366 the determination of the short-time response to external forcing (Abramov and Majda 2009).
367 Kernel methods can become computationally expensive, and they are inherently restricted to
368 low-dimensional applications. The ST/qG-FDT method of Abramov and Majda (2009) does
369 not suffer from this problem. It might be an option to be tested in the future. However, we
370 also speculate that, due to the central-limit theorem, the deviations from Gaussianity might
371 become the smaller the more complex, and thus realistic, the examined setting becomes.
372 The ability of the qG-FDT to predict the response of the SGS parameterizations has been
373 investigated using the example of anomalous local vorticity forcings in midlatitudes, at twelve
374 different equidistant positions in geographic longitude, and projected on the EOF bases which
375 the corresponding low-order models use. It is found that qG-FDT can predict the response
376 in the first moments of the toy-atmosphere climate well, not however that of the second
377 moments. This is in line with the findings of Majda et al. (2005) that, for systems with

378 quadratic nonlinearity, use of a Gaussian PDF in (21) yields third-order accurate results for
379 the first moments, while those for the second moments are second-order accurate. Indeed
380 Gritsun et al. (2008) found a worse, albeit reasonable, qG-FDT performance for second than
381 for first moments. Moreover, the forcing chosen here is sub-optimal, as Abramov and Majda
382 (2009) show that ST/qG-FDT applied to this system works best for anomalous forcings
383 projecting onto the leading EOF 1. This is no real surprise since the toy-atmosphere with
384 its 231 degrees of freedom is only roughly consistent with the basic assumptions of the
385 FDT. Only barotropic Rossby waves are present. Neither does the toy atmosphere allow
386 comparatively fast synoptic-scale processes such as baroclinic instability, nor does it contain
387 gravity waves. Thus a basic picture of slow modes stochastically forced by components with
388 much shorter intrinsic time scales is not met very well so that the system PDF could have a
389 stronger fractality than allowed under ideal conditions. Corresponding extensions should be
390 considered in the future. In the present context, however, the reliable qG-FDT prediction
391 of the changes in the first moments can be used to predict the response of the SGS forcing
392 to the external forcing. In an approach which we call reduced qG-FDT (rqG-FDT) this has
393 been done while the linear SGS operator has been kept untouched.

394 The reduced qG-FDT has then been applied to the various anomalous-forcing cases.
395 Low-order models with SGS closure adjusted via rqG-FDT have been investigated for their
396 ability in predicting first- and second-moment anomalies in the data of the perturbed toy
397 atmosphere. This has been compared to the potential of low-order models without adjusted
398 parameterization, or of the direct application of qG-FDT. Only very small models, based
399 on only 20 EOFs, perform worse than qG-FDT. With a basis of intermediate size (30 –
400 60 EOFs) they are more successful in predicting the second-moment anomalies, i.e. the
401 anomalous fluxes, while direct application of qG-FDT. gives a more reliable prediction of
402 the first-moment anomalies, i.e. the anomalous streamfunction. There, however, rqG-FDT is
403 already able to improve the low-order model prediction, as compared to simulations without
404 modified SGS parameterization. An encouraging result is that models based on sufficiently

405 many EOFs (80 or 90) perform clearly best if adjusted via rqG-FDT. Both first- and second-
406 moment anomalies are simulated better (by about 30% for second moments) than by models
407 without adjusted parameterization, or (by even more) than by the direct application of the
408 qG-FDT.

409 It thus seems that the combination of FDT and explicit simulations of the nonlinear
410 system is a promising approach which should be pursued further. Another promising route
411 specifically towards realistic low-order modelling of the atmospheric climate could perhaps
412 be the combination of a reduced stochastic model with non-Gaussian FDT. At least for
413 a three-component system Majda et al. (2010) show this approach to be significantly more
414 powerful than the application of qG-FDT to the complete system. One might also reconsider
415 the tuning process for the SGS parameterization by using concepts from information theory
416 (Majda and Gershgorin 2010, 2011a,b; Branicki and Majda 2012). However, given the en-
417 couraging results we have here we see our comparatively simple approach as supplementary
418 to such ideas. Interesting here is also that low-order models with SGS parameterization de-
419 termined directly from anomalous data of the toy atmosphere were performing even better
420 than all other models. This indicates that more general FDT approaches not relying on
421 quasi-Gaussianity (Abramov and Majda 2009; Cooper and Haynes 2011) could yield better
422 results. It also indicates, however that as soon as the FDT as a whole is better able to also
423 predict the second-moment anomalies, its application to the adjustment of the SGS parame-
424 terization might lead to even more useful results. We hope that this will be borne out in the
425 future when the approach will have been applied to toy atmospheres, or even real climate
426 data, with a better time-scale separation between slow and fast processes as here. Baroclinic
427 models, allowing for baroclinic instability, or unbalanced models, containing gravity waves,
428 will be interesting testbeds to be examined. As a corresponding encouragement we see the
429 findings of Gritsun et al. (2008) where in an application of qG-FDT to GCM data even the
430 second-moment results were quite reasonable.

431 *Acknowledgments.*

432 We gratefully acknowledge support by F. Selten, who allowed us to use his spectral code,
433 and by C. Franzke, who provided us with his empirical forcing. Comments by A. Majda
434 and an anonymous reviewer helped a lot in improving the manuscript. AG acknowledges
435 support by the Russian Ministry for Sciences and Education (project 14.740.11.0639).

REFERENCES

- 438 Abramov, R. V. and A. J. Majda, 2009: New algorithms for low-frequency climate response.
439 *J. Atmos. Sci.*, **66**, 286–309.
- 440 Achatz, U. and G. Branstator, 1999: A two-layer model with empirical linear corrections and
441 reduced order for studies of internal climate variability. *J. Atmos. Sci.*, **56**, 3140–3160.
- 442 Achatz, U. and J. D. Opsteegh, 2003a: Primitive-equation-based low-order models with
443 seasonal cycle. Part I: Model construction. *J. Atmos. Sci.*, **60**, 465–477.
- 444 Achatz, U. and J. D. Opsteegh, 2003b: Primitive-equation-based low-order models with sea-
445 sonal cycle. Part II: Application to complexity and nonlinearity of large-scale atmosphere
446 dynamics. *J. Atmos. Sci.*, **60**, 478–490.
- 447 Achatz, U. and G. Schmitz, 1997: On the closure problem in the reduction of complex
448 atmospheric models by PIPs and EOFs: A comparison for the case of a two-layer model
449 with zonally symmetric forcing. *J. Atmos. Sci.*, **54**, 2452–2474.
- 450 Achatz, U., G. Schmitz, and K.-M. Greisiger, 1995: Principal interaction patterns in baro-
451 clinic wave life cycles. *J. Atmos. Sci.*, **52**, 3201–3213.
- 452 Branicki, M. and A. Majda, 2012: Quantifying uncertainty for predictions with model error
453 in non-gaussian systems with intermittency. *Nonlinearity*, **25**, 2543–2578.
- 454 Charney, J. G., 1948: On the scale of atmospheric motion. *Geofys. Publ. Oslo*, **17**, 1–17.
- 455 Cooper, F. C. and P. H. Haynes, 2011: Climate sensitivity via a nonparametric fluctuation-
456 dissipation theorem. *J. Atmos. Sci.*, **68**, 937–953.

- 457 Deker, U. and F. Haake, 1975: Fluctuation-dissipation theorems for classical processes. *Phys.*
458 *Rev. A*, **11**, 2043–2056.
- 459 Dolapchiev, S., U. Achatz, and I. Timofeyev, 2012: Stochastic closure for local averages in
460 the finite-difference discretization of the forced burgers equation. *Theor. Comput. Fluid*
461 *Dyn*, doi:10.1007/s00162-012-0270-1.
- 462 Durran, D., 1989: Improving the anelastic approximation. *J. Atmos. Sci.*, **46**, 1453–1461.
- 463 Farrell, B. F. and P. J. Ioannou, 1993: Transient development of perturbations in stratified
464 shear flow. *J. Atmos. Sci.*, **50**, 2201—2214.
- 465 Farrell, B. F. and P. J. Ioannou, 1996a: Generalized stability theory. Part I: Autonomous
466 operators. *J. Atmos. Sci.*, **53**, 2025—2040.
- 467 Farrell, B. F. and P. J. Ioannou, 1996b: Generalized stability theory. Part II: Nonautonomous
468 Operators. *J. Atmos. Sci.*, **53**, 2041–2053.
- 469 Franzke, C. and A. J. Majda, 2006: Low-order stochastic mode reduction for a prototype
470 atmospheric GCM. *J. Atmos. Sci.*, **63**, 457–479.
- 471 Franzke, C., A. J. Majda, and E. Vanden-Eijnden, 2005: Low-order stochastic mode reduc-
472 tion for a realistic barotropic model climate. *J. Atmos. Sci.*, **62**, 1722–1745.
- 473 Gritsun, A. and G. Branstator, 2007: Climate response using a three-dimensional operator
474 based on the fluctuation-dissipation theorem. *J. Atmos. Sci.*, **64**, 2558–2575.
- 475 Gritsun, A., G. Branstator, and A. Majda, 2008: Climate response of linear and quadratic
476 functionals using the fluctuation-dissipation theorem. *J. Atmos. Sci.*, **65**, 2824–2841.
- 477 Gritsun, A. S., 2001: Fluctuation-dissipation theorem on the attractors of atmospheric mod-
478 els. *Russ. J. Numer. Analysis Math. Modell.*, **16**, 115–133.

479 Gritsun, A. S., G. Branstator, and V. P. Dymnikov, 2002: Construction of the linear response
480 operator of an atmospheric general circulation model to small external forcing. *Russ. J.*
481 *Numer. Anal. Math. Modell.*, **17**, 399416.

482 Hänggi, P. and H. Thomas, 1977: Time evolution, correlations and linear response of non-
483 Markov processes. *Z. Phys.*, **26B**, 85–92.

484 Hasselmann, K., 1976: Stochastic climate models, Part 1: Theory. *Tellus*, **28**, 473 – 485.

485 Held, I. M., 2005: The gap between simulation and understanding in climate modeling. *Bull.*
486 *Amer. Meteor. Soc.*, **86**, 1609–1614, doi:10.1175/BAMS-86-11-1609.

487 Kraichnan, R. H., 1959: Classical fluctuation-relaxation theorem. *Phys. Rev.*, **113**, 1181–
488 1182.

489 Kwasniok, F., 1996: The reduction of complex dynamical systems using principal interaction
490 patterns. *Physica D*, **92**, 28–60.

491 Kwasniok, F., 2004: Empirical low-order models of barotropic flow. *J. Atmos. Sci.*, **61**,
492 235–245.

493 Kwasniok, F., 2007: Reduced atmospheric models using dynamically motivated basis func-
494 tions. *J. Atmos. Sci.*, **64**, 3452–3474.

495 Lipps, F., 1990: On the anelastic approximation for deep convection. *J. Atmos. Sci.*, **47**,
496 1794–1798.

497 Lipps, F. and R. Hemler, 1982: A scale analysis of deep moist convection and some related
498 numerical calculations. *J. Atmos. Sci.*, **29**, 2192–2210.

499 Lorenz, D. J. and E. T. DeWeaver, 2007: Tropopause height and zonal wind response to
500 global warming in the IPCC scenario integrations. *J. Geophys. Res.*, **112**, D10 119, doi:
501 10.1029/2006JD008087.

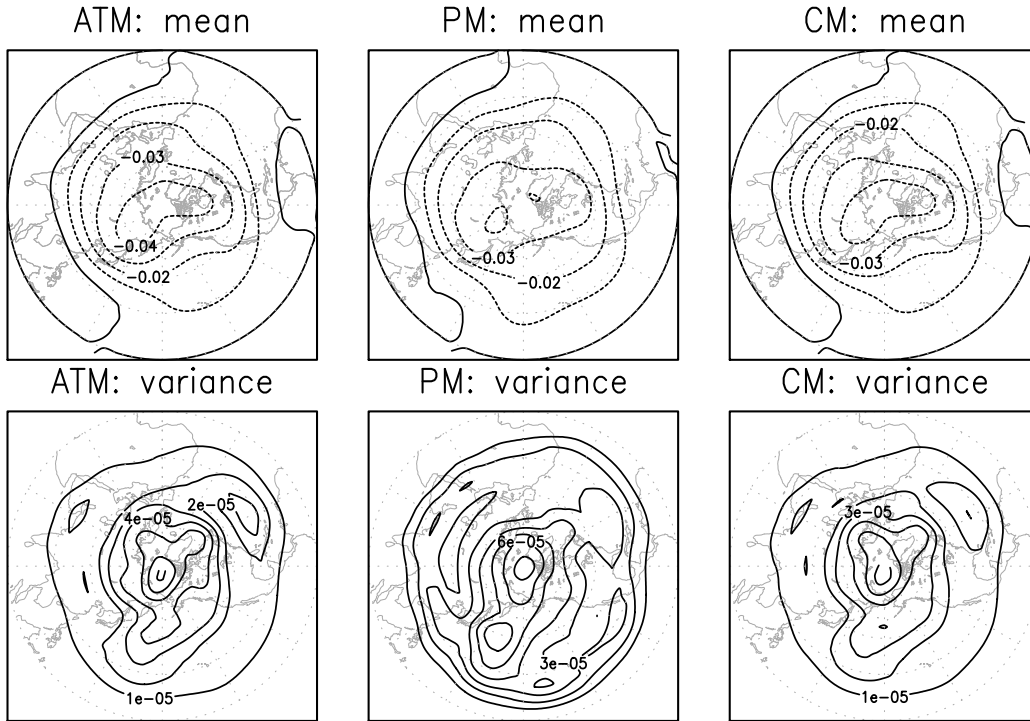
- 502 Majda, A., R. Abramov, and M. Grote, 2005: Information theory and stochastics for multi-
503 scale nonlinear systems. *CRM Monogr. Series*, **25**, 1–133.
- 504 Majda, A. and B. Gershgorin, 2010: Quantifying uncertainty in climate change science
505 through empirical information theory. *Proc. Natl. Acad. Sci.*, **107**, 14 958–14 963.
- 506 Majda, A. and B. Gershgorin, 2011a: Improving model fidelity and sensitivity for complex
507 systems through empirical information theory. *Proc. Natl. Acad. Sci.*, **108**, 10 044–10 049.
- 508 Majda, A. and B. Gershgorin, 2011b: Link between statistical equilibrium fidelity and fore-
509 casting skill for complex systems with model error. *Proc. Natl. Acad. Sci.*, **108**, 12 599–
510 12 5604.
- 511 Majda, A., B. Gershgorin, and Y. Yuan, 2010: Low frequency climate response and
512 fluctuation- dissipation theorems: theory and practice. *J Atmos Sci.*, **67**, 1186–1201.
- 513 Majda, A. J., I. Timofeyev, and E. Vanden-Eijnden, 2003: Systematic strategies for stochas-
514 tic mode reduction in climate. *J. Atmos. Sci.*, **60**, 1705–1722.
- 515 Ogura, Y. and N. A. Phillips, 1962: A scale analysis of deep and shallow convection in the
516 atmosphere. *J. Atmos. Sci.*, **19**, 173–179.
- 517 Opsteegh, J., R. Haarsma, F. Selten, and A. Kattenberg, 1998: ECBILT: a dynamic alter-
518 native to mixed boundary conditions in ocean models. *Tellus A*, **50 (3)**, 348–367, URL
519 <http://www.tellusa.net/index.php/tellusa/article/view/14524>.
- 520 Petoukhov, V., A. Ganopolski, V. Brovkin, M. Claussen, A. Eliseev, C. Kubatzki, and
521 S. Rahmstorf, 2000: CLIMBER-2: a climate system model of intermediate complexity.
522 Part I: model description and performance for present climate. *Clim. Dyn.*, **16**, 1–17.
- 523 Phillips, N., 1954: Energy transformations and meridional circulations associated with simple
524 baroclinic waves in a two-level, quasi-geostrophic model. *Tellus*, **6**, 273–286.

- 525 Phillips, N., 1956: The general circulation of the atmosphere: a numerical experiment.
526 *Quart. J. R. Met. Soc.*, **82**, 123–164.
- 527 Phillips, N. A., 1963: Geostrophic motion. *Rev. Geophys.*, **1(2)**, 123176, doi:10.1029/
528 RG001i002p00123.
- 529 Risken, H., 1984: *The Fokker-Plank Equation. Methods of Solution and Applications.*
530 Springer-Verlag, 474 pp.
- 531 Robinson, A. and H. Stommel, 1959: The oceanic thermocline and the associated thermo-
532 haline circulation. *Tellus*, **11**, 295–308.
- 533 Selten, F. M., 1995: An efficient description of the dynamics of barotropic flow. *J. Atmos.*
534 *Sci.*, **52**, 915–936.
- 535 Selten, F. M., 1997: Baroclinic empirical orthogonal functions as basis functions in an at-
536 mospheric model. *J. Atmos. Sci.*, **54**, 2100–2114.
- 537 Voss, R., R. Saussen, and U. Cubasch, 1998: Periodically synchronously coupled integrations
538 with the atmosphere-ocean general circulation model ECHAM3/LSG. *Climate Dyn.*, **14**,
539 249–266.
- 540 Welander, P., 1959: An advective model of the ocean thermocline. *Tellus*, **11**, 309–318.
- 541 Zeeman, E. C., 1988: Stability of dynamical systems. *Nonlinearity*, **1**, 115–155.

542 List of Figures

- 543 1 Mean streamfunction (top row, contour interval 0.01) and streamfunction vari-
544 ance (bottom, contour interval $1 \cdot 10^{-5}$), from 200000d of data from the toy
545 atmosphere (left column), a projected 40-EOF model without SGS parame-
546 terization (middle), and a 40-EOF climate model with SGS parameterization
547 (right). The streamfunction has been normalized by $a^2\Omega$ with Ω the angular
548 frequency of the earth. 28
- 549 2 Vorticity forcing (bottom row, contour interval $1 \cdot 10^{-3}$, only negative contours
550 shown) and corresponding streamfunction forcing (top, contour interval $2 \cdot$
551 10^{-5}), centered at $(\lambda_c, \phi_c) = (180^\circ, 45^\circ)$, and nondimensionalized by length
552 scale a and time scale Ω^{-1} . Shown are the total forcing (left column), the
553 results one obtains from projection onto the leading 40 EOFs (middle), and
554 the result for 90 EOFs (right). 29
- 555 3 Relative error in using quasi-Gaussian FDT (qG-FDT) for predicting the re-
556 sponse of the toy atmosphere to anomalous local forcing at twelve different
557 longitudes, and projected onto the leading 40 EOFs. Errors have been calcu-
558 lated for the response in the mean reduced state $\langle \mathbf{a} \rangle$, the mean SGS error $\langle \mathbf{s} \rangle$,
559 the covariance of the SGS error with the reduced state vector $\langle \mathbf{s}' \mathbf{a}'^t \rangle$, and the
560 reduced auto-covariance $\langle \mathbf{a}' \mathbf{a}'^t \rangle$. The qG-FDT operator is based on 40 EOFs
561 as well. 30
- 562 4 For the same twelve cases as discussed in Fig. 3, the relative error between
563 the estimates from qG-FDT for the linear operator and forcing of the SGS
564 parameterization of a 40-EOF climate model and the à-posteriori result from
565 the perturbed atmosphere itself. Also shown is the forcing error in applying
566 the reduced qG-FDT (rqG-FDT) as explained in the main text. 31

567	5	The mean streamfunction of the toy atmosphere (upper left panel), its re-	
568		sponse to an anomalous vorticity forcing at longitude $\lambda_c = 210^\circ$, projected	
569		onto 90 EOFs (lower left), the simulation of this response by a 90-EOF climate	
570		model with unmodified SGS parameterization (upper middle), by a climate	
571		model with SGS parameterization corrected à-posteriori by investigation of	
572		the perturbed atmosphere (lower middle), by a climate model with SGS pa-	
573		rameterization corrected by rqG-FDT (upper right), and the direct estimation	
574		of the streamfunction response by qG-FDT (lower right). All values have been	
575		normalized by $a^2\Omega$, and the response has been multiplied by a factor 10.	32
576	6	As Fig. 5, but now for the zonal wind. Units are m/s.	33
577	7	As Fig. 5, but now for the streamfunction variance. All values have been	
578		normalized by $a^4\Omega^2$, and the response has been multiplied by a factor 5.	34
579	8	Relative error in predicting the first-moment response of the toy atmosphere	
580		to anomalous local forcing at twelve different longitudes, and projected onto	
581		the leading 90 EOFs. Models used for the prediction are a 90-EOF low-	
582		order climate model with SGS parameterization obtained from unperturbed	
583		reference data (model CM0 in Figs. 5 - 7), a model with SGS parameterization	
584		adjusted à-posteriori on the basis of perterbed atmosphere data (model CMP	
585		in Figs. 5 - 7), a model using rqG-FDT for a before-hand prediction of the	
586		necessary change in the SGS parameterization (model CMF in Figs. 5 - 7),	
587		and direct application of qG-FDT.	35
588	9	As Fig. 8, but now the relative error in predicting the second-moment response	
589		of the toy atmosphere. Note the logarithmic scale.	36
590	10	For the same models as also analyzed in Fig. 8, now however at resolutions,	
591		i.e. number of basic EOFs, between 20 and 90, the mean first-moment error	
592		plus/minus the root-mean-square deviation, obtained from all twelve forcing	
593		cases, respectively.	37



40 EOFs

FIG. 1. Mean streamfunction (top row, contour interval 0.01) and streamfunction variance (bottom, contour interval $1 \cdot 10^{-5}$), from 200000d of data from the toy atmosphere (left column), a projected 40-EOF model without SGS parameterization (middle), and a 40-EOF climate model with SGS parameterization (right). The streamfunction has been normalized by $a^2\Omega$ with Ω the angular frequency of the earth.

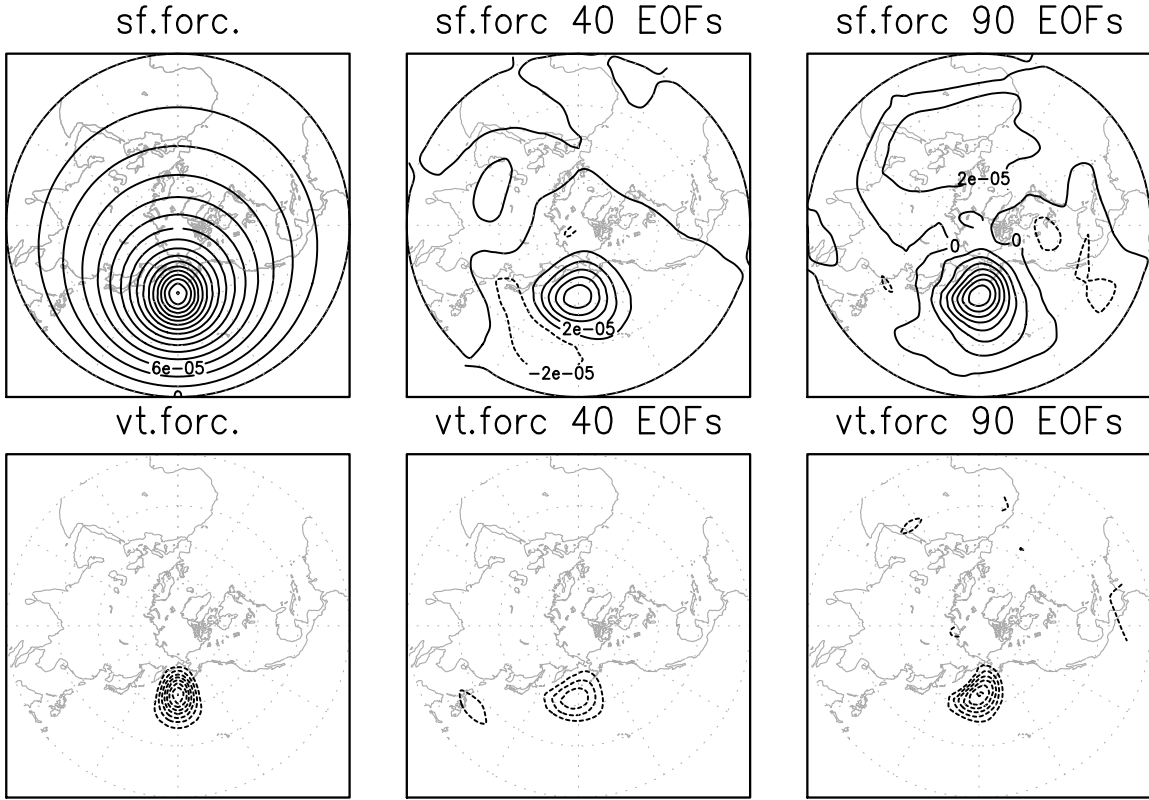


FIG. 2. Vorticity forcing (bottom row, contour interval $1 \cdot 10^{-3}$, only negative contours shown) and corresponding streamfunction forcing (top, contour interval $2 \cdot 10^{-5}$), centered at $(\lambda_c, \phi_c) = (180^\circ, 45^\circ)$, and nondimensionalized by length scale a and time scale Ω^{-1} . Shown are the total forcing (left column), the results one obtains from projection onto the leading 40 EOFs (middle), and the result for 90 EOFs (right).

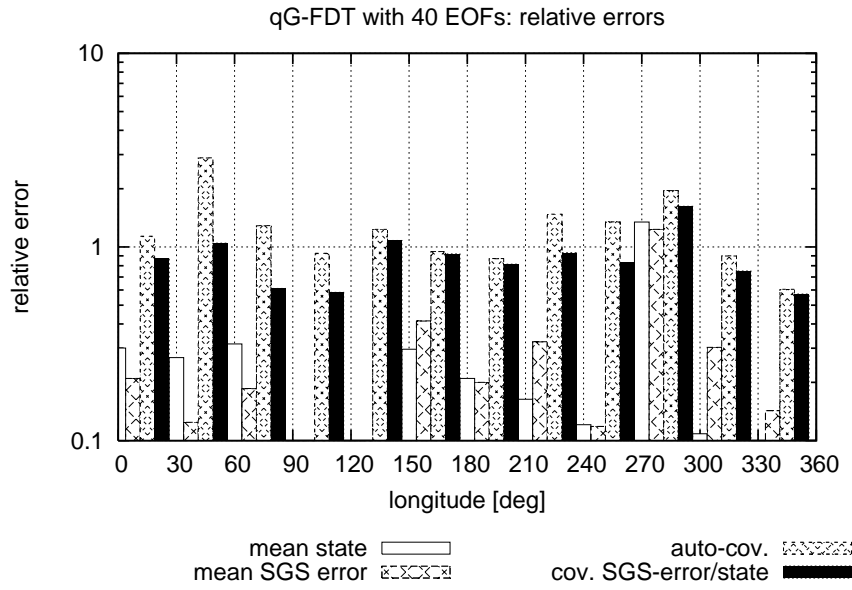


FIG. 3. Relative error in using quasi-Gaussian FDT (qG-FDT) for predicting the response of the toy atmosphere to anomalous local forcing at twelve different longitudes, and projected onto the leading 40 EOFs. Errors have been calculated for the response in the mean reduced state $\langle \mathbf{a} \rangle$, the mean SGS error $\langle \mathbf{s} \rangle$, the covariance of the SGS error with the reduced state vector $\langle \mathbf{s}' \mathbf{a}'^t \rangle$, and the reduced auto-covariance $\langle \mathbf{a}' \mathbf{a}'^t \rangle$. The qG-FDT operator is based on 40 EOFs as well.

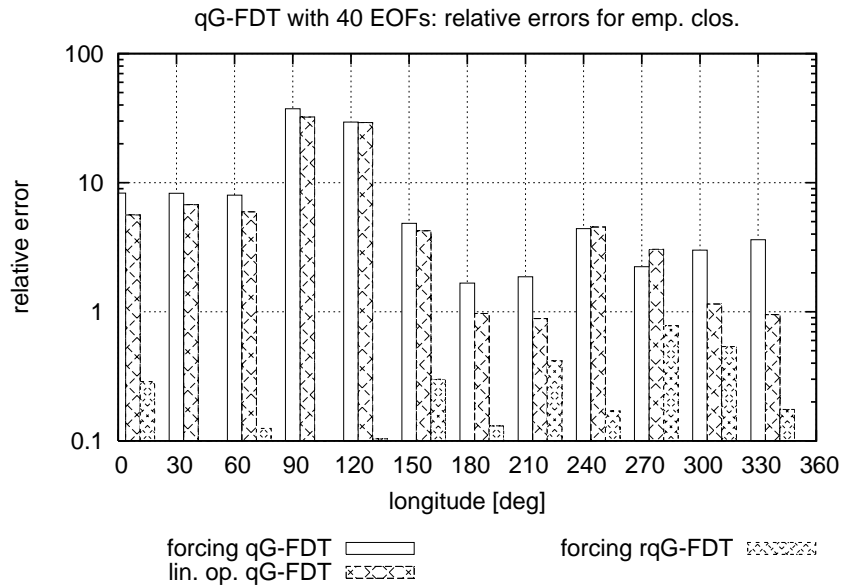
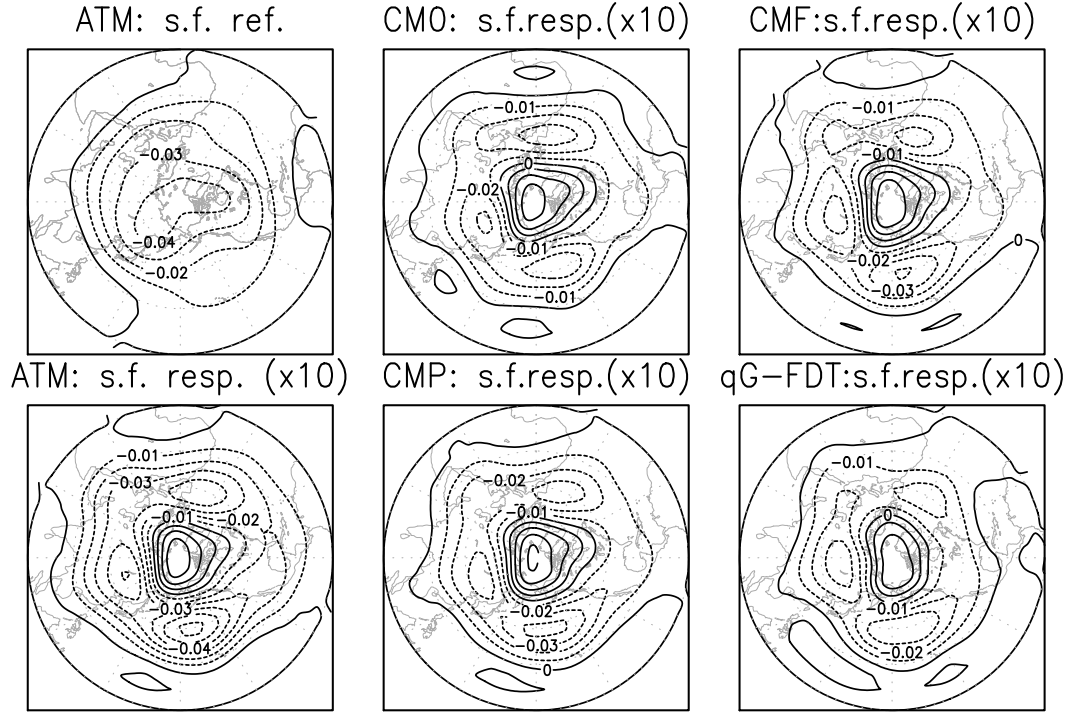
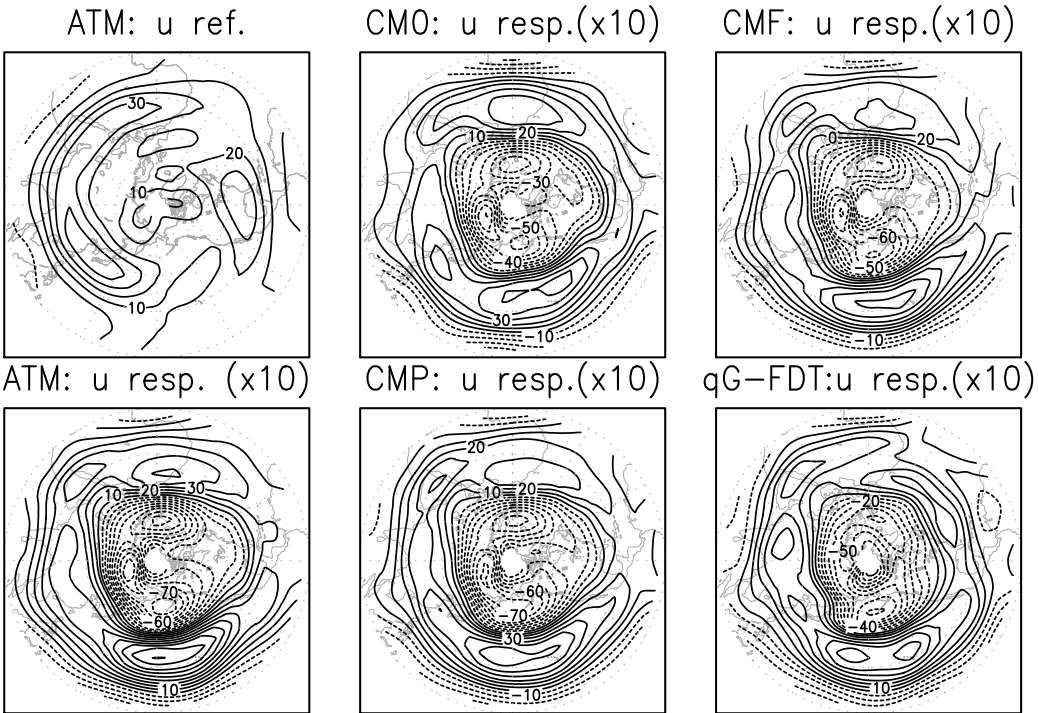


FIG. 4. For the same twelve cases as discussed in Fig. 3, the relative error between the estimates from qG-FDT for the linear operator and forcing of the SGS parameterization of a 40-EOF climate model and the à-posteriori result from the perturbed atmosphere itself. Also shown is the forcing error in applying the reduced qG-FDT (rqG-FDT) as explained in the main text.



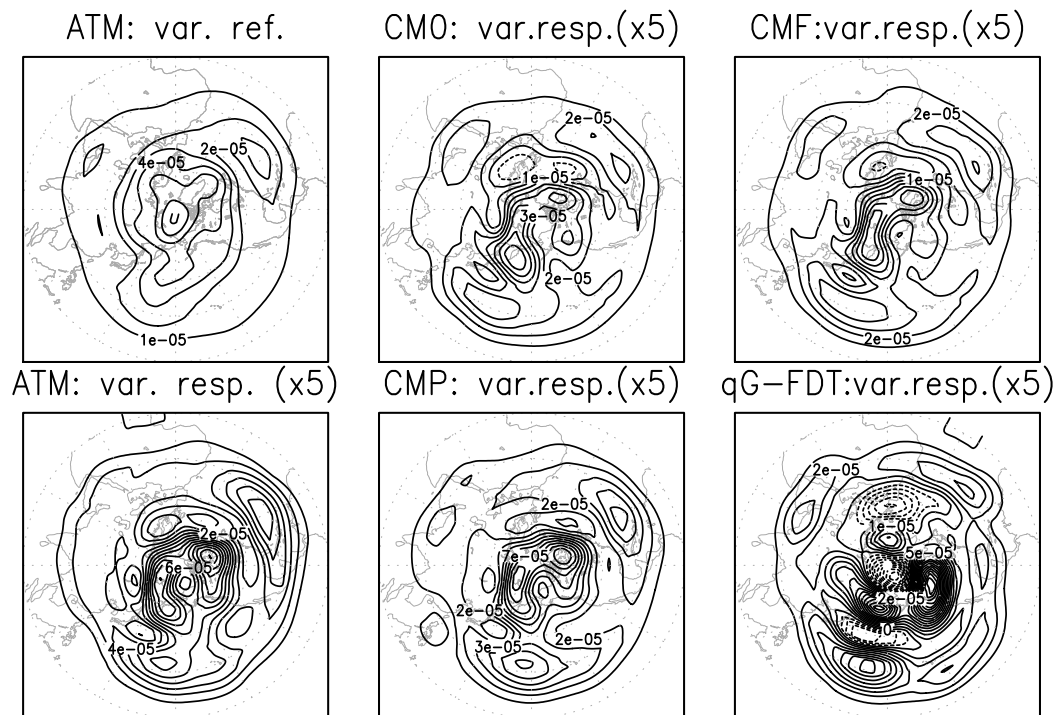
pert. at lon = 210 using 90 EOFs

FIG. 5. The mean streamfunction of the toy atmosphere (upper left panel), its response to an anomalous vorticity forcing at longitude $\lambda_c = 210^\circ$, projected onto 90 EOFs (lower left), the simulation of this response by a 90-EOF climate model with unmodified SGS parameterization (upper middle), by a climate model with SGS parameterization corrected à-posteriori by investigation of the perturbed atmosphere (lower middle), by a climate model with SGS parameterization corrected by rqG-FDT (upper right), and the direct estimation of the streamfunction response by qG-FDT (lower right). All values have been normalized by $a^2\Omega$, and the response has been multiplied by a factor 10.



pert. at lon = 210 using 90 EOFs

FIG. 6. As Fig. 5, but now for the zonal wind. Units are m/s.



pert. at lon = 210 using 90 EOFs

FIG. 7. As Fig. 5, but now for the streamfunction variance. All values have been normalized by $a^4\Omega^2$, and the response has been multiplied by a factor 5.

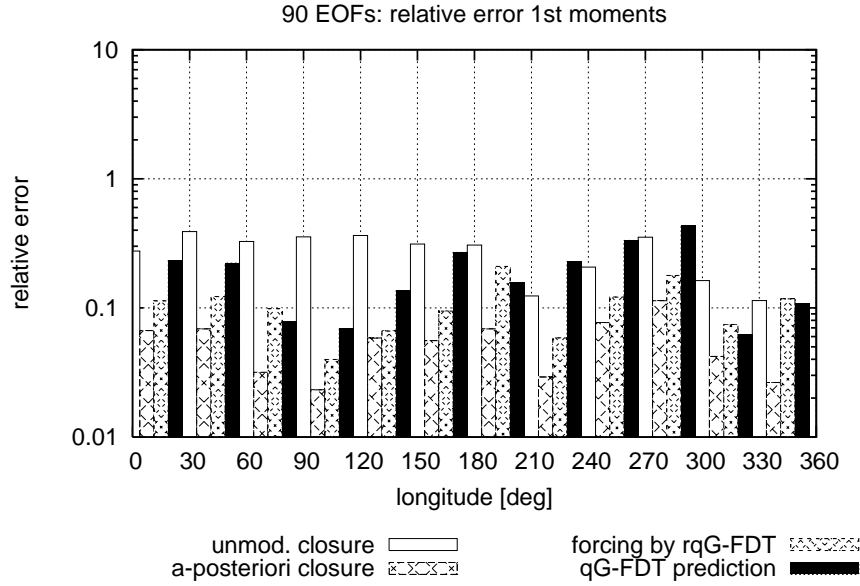


FIG. 8. Relative error in predicting the first-moment response of the toy atmosphere to anomalous local forcing at twelve different longitudes, and projected onto the leading 90 EOFs. Models used for the prediction are a 90-EOF low-order climate model with SGS parameterization obtained from unperturbed reference data (model CM0 in Figs. 5 - 7), a model with SGS parameterization adjusted a-posteriori on the basis of perturbed atmosphere data (model CMP in Figs. 5 - 7), a model using rqG-FDT for a before-hand prediction of the necessary change in the SGS parameterization (model CMF in Figs. 5 - 7), and direct application of qG-FDT.

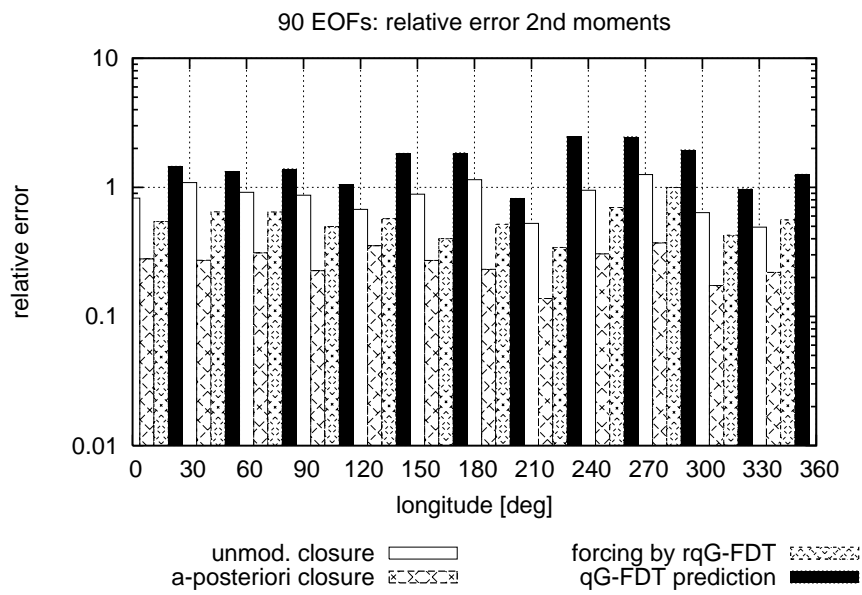


FIG. 9. As Fig. 8, but now the relative error in predicting the second-moment response of the toy atmosphere. Note the logarithmic scale.

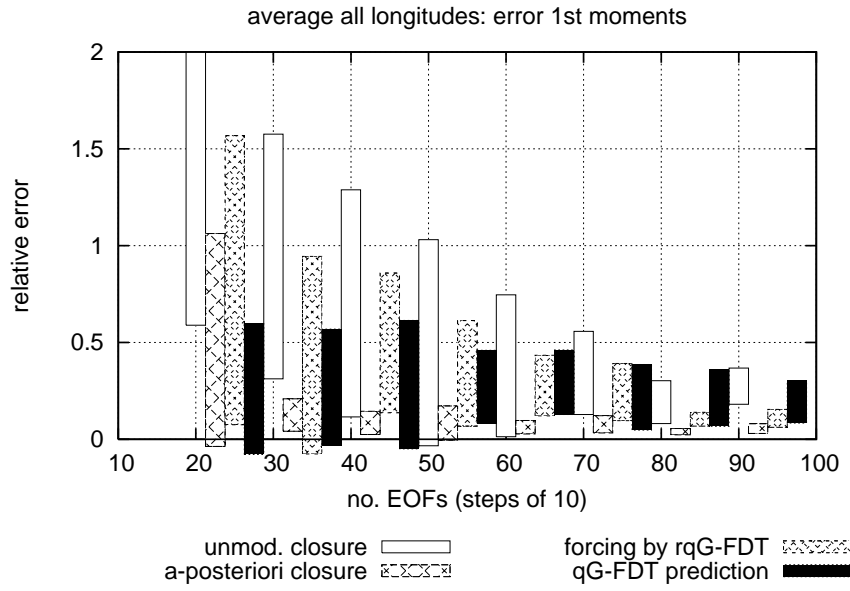


FIG. 10. For the same models as also analyzed in Fig. 8, now however at resolutions, i.e. number of basic EOFs, between 20 and 90, the mean first-moment error plus/minus the root-mean-square deviation, obtained from all twelve forcing cases, respectively.

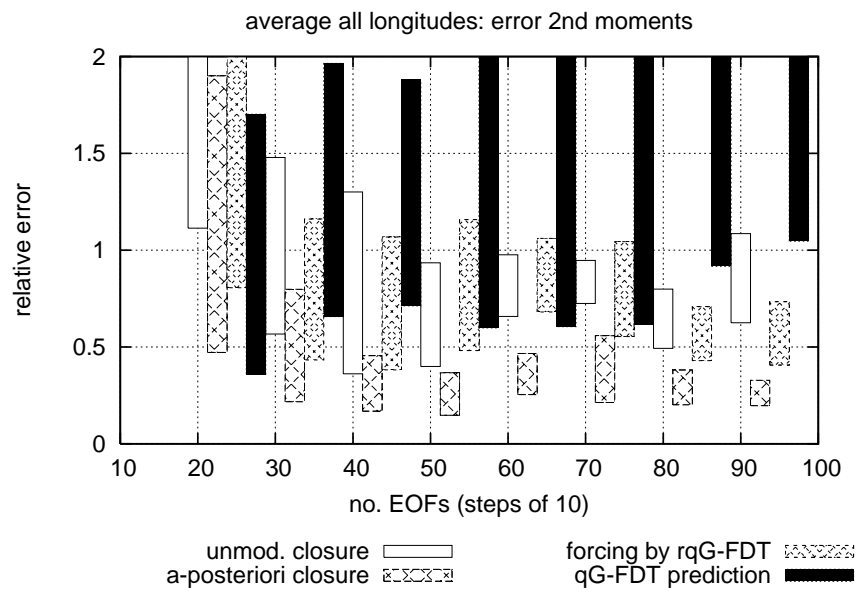


FIG. 11. As Fig. 10, but now for the second-moment errors.